Paper:

Needle Tip Position Accuracy Evaluation Experiment for Puncture Robot in Remote Center Control

Kohei Sugiyama[*1], **Takayuki Matsuno**[*1], **Tetsushi Kamegawa**[*1], **Takao Hiraki**[*2], **Hirotaka Nakaya**[*1], **Masayuki Nakamura**[*3], **Akira Yanou**[*4], **and Mamoru Minami**[*1]

[*1]Graduate School of Natural Science and Technology, Okayama University
3-1-1 Tsushimanaka, Kita-ku, Okayama city, Okayama 700-8530, Japan
E-mail: en422839@s.okayama-u.ac.jp
[*2]Department of Radiology, Okayama University Hospital
2-5-1 Shikata, Kita-ku, Okayama city, Okayama 700-8558, Japan
[*3]Department of Mechanical Systems Engineering, Okayama University
3-1-1 Tsushimanaka, Kita-ku, Okayama city, Okayama 700-8530, Japan
[*4]Department of Radiological Technology, Kawasaki College of Allied Health Professions
316 Matsushima, Kurashiki, Okayama 701-0194, Japan
[Received January 25, 2016; accepted October 10, 2016]

In recent years, a medical procedure called interventional radiology (IR) has been attracting considerable attention. Doctors can perform IR percutaneously while observing the fluoroscopic image of patients. Therefore, this surgical method is less invasive. In this surgery, computed tomography (CT) equipment is often used for precise fluoroscopy. However, doctors are exposed to strong radiation from the CT equipment. In order to overcome this problem, we have developed a remote-controlled surgical assistance robot called Zerobot. In animal puncture experiment, the operation of Zerobot was based on joint control. Therefore, during a surgery, the tip of the needle moves when a surgeon orders for a change in the direction of the needle. This makes the robot less user-friendly because the surgeon tracks the trajectory of the tip of the needle. This problem can be solved by using remote center control.

Keywords: surgical assistance robot, interventional radiology, puncture robot

1. Introduction

Interventional radiology (IR) is a surgical method conducted with imaging modalities such as computed tomography (CT) and X-rays. A surgeon conducts IR percutaneously by inserting a needle or a catheter into body of a patient while observing medical images of the patient. In particular, the CT equipment has high visibility and objectivity. CT fluoroscopy systems, which can show medical images in real-time, are superior as guiding tools for IR. Therefore, CT-guided IR is used in lung cancer treatment, liver cancer treatment, biopsy, etc. [1]. The manual IR treatment is illustrated in **Fig. 1**. When compared to the conventional methods, IR can be conducted under local anesthesia and is minimally invasive. Moreover, patients can be discharged from the hospital within three or four days after the treatment. Because of these advantages, IR is paid much attention in recent years. According to clinical data, the minimum size of malignancy is approximately 3 mm in diameter [2]. Therefore, surgeons must puncture such small malignant tumors carefully and accurately by using needles. In addition, surgeons are exposed to radiation during CT scanning because they conduct the procedure close to the CT gantry.

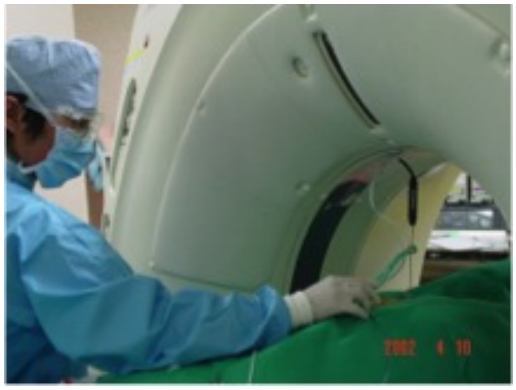

Fig. 1. Interventional radiology.

In order to prevent radiation exposure, surgeons wear radiation protection aprons and hold needles using forceps; this creates a distance between the hand and the CT radiography plane. However, it is impossible to prevent radiation exposure completely. Medical robots and IR training systems, such as AcuBot [3], CT-Bot [4], MAXIO [5], and others [6, 7], are developed in order to improve the positioning accuracy of needles and to reduce radiation exposure. These robots assist the surgeons in inserting a needle during a CT-guided puncture. However, Zerobot, which is developed by us, assists the surgeon throughout the process (from positioning the robot

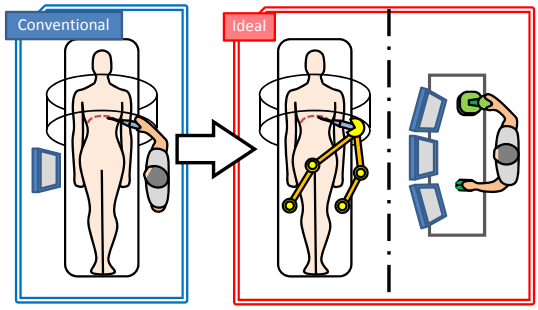

Fig. 2. Concept of robotic IR.

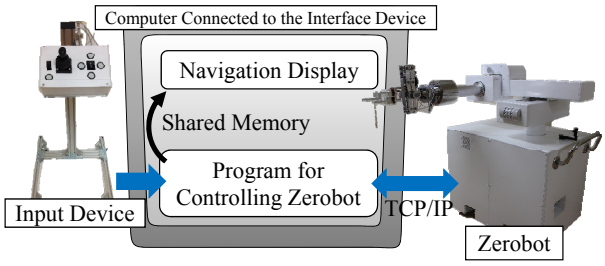

Fig. 3. System structure of robotic IR.

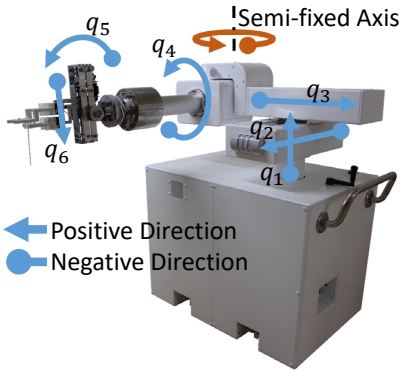

Fig. 4. Appearance of Zerobot.

to inserting a needle) by remote control.

In this research, in order to confirm the problems with robotic IR systems, we conducted a phantom puncture experiment [8] and an animal puncture experiment [9]. From these experiments, it was confirmed that adjusting the position of the needle without changing the position of the tip of the needle is troublesome. This is because the tip of the needle moves when a surgeon orders a change in the direction of the needle. In order to solve this problem, remote center control should be adjusted into Zerobot. Remote center control is a method in which some active joints are controlled synchronously in order to set the center of rotation to an arbitrary point. If center of rotation is set as the tip of the needle, the needle posture can be changed without changing the position of the tip of the needle. Thus, in this control method, Zerobot simplifies the procedure of the IR surgery. In AcuBot, remote center control is implemented by using a mechanical structure called MINI-RCM. MINI-RCM adapts to various needles by adjusting an RCM point, which is the needle pivoting point, during the needle orientation. However, during needle insertion, the RCM point cannot be changed actively from the needle entry point because the point is constrained by the mechanical structure, which is manually preset. From our animal experiment, it is confirmed that the needle deflects when inserted into a living body. In that case, surgeons have to orient the posture of the needles frequently for eliminating the deflection of the needles. We assumed that an optimal RCM point for decreasing the deflection of the needle and the body tissue is not only the needle entry point. Therefore, we implemented remote center control by calculating the positions of all the axes synchronously so that the RCM point can be changed actively.

According to the minimum size of malignancy, which is approximately 3 mm in diameter, we set the target positioning accuracy of the tip of the needle as 1.0 mm. Therefore Zerobot must archive the target accuracy if it was controlled by a remote center. Then, we conducted an experiment for evaluating the positioning accuracy of the tip of the needle in remote center control.

The concept of robotic IR is illustrated in **Fig. 2**. This paper presents an overview of the robotic IR and the result of the accuracy evaluation experiment. Section 2 describes the overview, which includes the mechanism of Zerobot, procedure of puncture, interface devices, and system structure. The forward and inverse kinematics of remote center control are derived in Section 3. In Section 4, an experiment for evaluating the positioning accuracy of the tip of the needle is explained. Finally, Section 5 concludes the paper.

2. Overview of Robotic IR

2.1. System Structure

This subsection describes the system structure of the robotic IR. The system configuration is illustrated in **Fig. 3**. Zerobot is connected to a computer, which is connected to an interface device using Ethernet. It communicates with the computer through TCP/IP. After receiving the status of the interface device, the computer instructs Zerobot to actuate the axes. Zerobot communicates the angle and displacement of six joints and the value obtained from the force sensor to the interface device. In the interface device, the process that controls the trajectory of Zerobot and the navigation display are segregated. The program that controls Zerobot receives the status of Zerobot. Then, the shared memory sends the status to the navigation display.

2.2. Mechanism

The appearance of Zerobot is shown in **Fig. 4**. It has five degrees of freedom (DOFs) for adjusting the position of the tip of the needle and the direction of the needle and

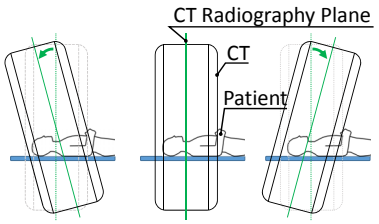

Fig. 5. Definition of CT radiography plane.

one DOF for varying the puncturing direction. Six actuators are included in the machine: four linear actuators (in the directions of X, Y, Z, and puncturing axes) and two rotational actuators (around the X and Y-axes). Three AC servomotors are used for the actuators corresponding to the X, Y, and Z-axes. Three DC servomotors are used for the actuators corresponding to the puncturing axis and around the X and Y-axes. All the motors have digital encoders. Therefore, Zerobot can perform a puncturing operation by actuating the puncturing axis regardless of the posture of the needle. Four wheels are attached to the bottom of the robot so that it can be moved by humans. During a surgery, the robot is fixed under the surgical bed by locking the wheels. The robot changes the direction of the needle and performs the puncturing operation in the CT gantry with its arm above the patient.

If metal parts are present in the gantry, incorrect images called artifacts will appear on the CT images because of a method that is used to reconstruct the images obtained by the CT equipment. If an artifact appears on the CT image, the internal image of the patient will not be clear, and this will cause inconvenience during the surgery. Therefore, metal parts cannot be used for manufacturing needle grippers. Accordingly, needle grippers are made of engineering plastic, which is a radiolucent material. The motor is used in the end effector for puncturing. In addition, the angle of elevation of the CT equipment can be changed as necessary, as shown in **Fig. 5**. A motor is required for adjusting the direction of the needle corresponding to the elevation angle of the CT equipment. Nevertheless, artifacts occur. These motors cannot be mounted near the needle gripper. Therefore, the motor used for puncturing and the motor used for changing the direction of the needle are located far from CT radiography plane by using a parallel link mechanism at the end effector, as shown in **Fig. 6**. The front part of the gripping needle is made of polyacetal. Two force sensors are located on the root of the needle gripper. These sensors can measure the moment around the three axes. Using these devices, the reaction force of the skin is calculated and analyzed.

2.3. Puncturing Procedure

This subsection describes the procedure of the robotic IR as follows.

1. Scanning Whole Abdomen:
   The target position of the tumor is confirmed using the CT image of the patient.

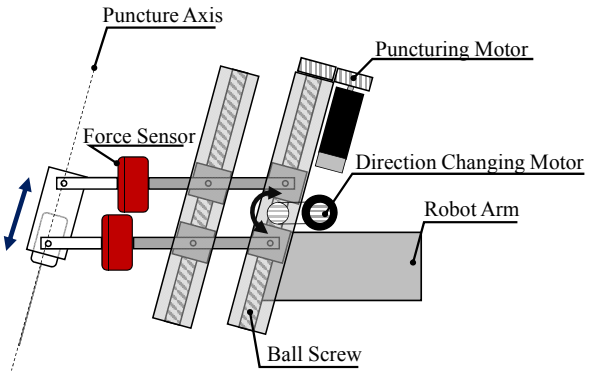

Fig. 6. End effector of Zerobot.

2. Planning:
   The relation between the catheter marker and the position of the tumor is confirmed by using the CT image, and the puncture path is planned. Then, a puncturing point is marked on the surface of the skin with a pen.

3. Adjustment of Needle Tip Position and Direction:
   A needle is brought to the CT radiography plane based on the laser emitted from the CT equipment. The position of the tip of the needle is adjusted to the marked position on the surface of the skin. Then, the direction of the needle is also adjusted to the preplanned angle.

4. Fine Adjustment of Needle Direction:
   Fine adjustments are made to the direction of the needle to direct the needle to the target tumor under CT guidance. Artifact from the needle can be regarded as an extension line of the needle.

5. Puncturing:
   The needle is punctured into the body. When the depth of the puncture is equal to the preplanned value, the surgeon confirms the relation between the position of the tip of the needle and the center of the tumor by observing CT radiography. Then, either the position of the tip of the needle or the direction of the needle is readjusted as necessary.

Zerobot is used in the above-mentioned sequence. If the robot cannot manipulate the needle accurately, the surgeon has to readjust the posture of the needle based on the real-time CT image. This increases the radiation exposure of the patient. Therefore, the positioning accuracy of the robotic hand should be improved.

2.4. Interface System

The design of the interface device is important for the safe operation because the doctor remotely operates Zerobot. The developed interface device is shown in the left side of **Fig. 3**. This interface consists of nine push buttons and a joystick. The right half of the input panel, which is further to the right side of the joystick, corresponds to

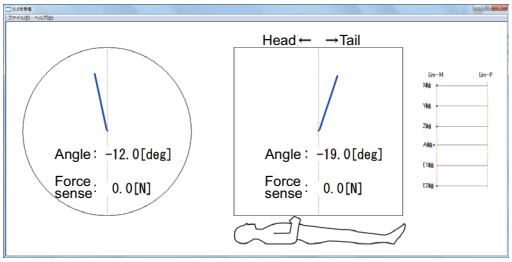

Fig. 7. Appearance of navigation display.

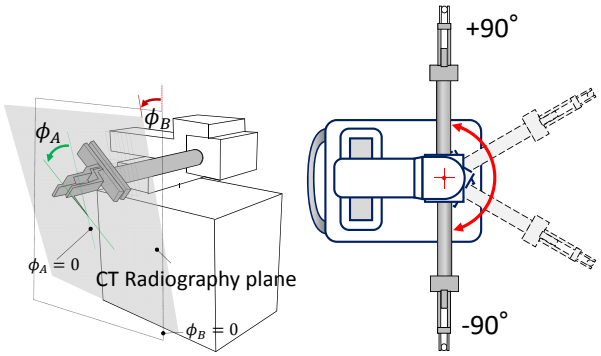

Fig. 8. Important kinematic parameters. Left side defines ϕ_A and ϕ_B and right side indicates the posture that can be taken by the semi-fixed axis.

the actuation of the linear axes, X, Y, and Z, of Zerobot. On the other hand, the left half of the input panel, which includes the joystick, corresponds to the rotation around the X and Y-axes and actuation axis of the puncture. The speed of the actuator is switchable so that the speed of the needle puncture can be increased when the needle penetrates the surface of the skin. **Fig. 3** shows the interface device fixed on a special stand. In addition, the device can be detached from the stand and used at any position at which the length of the connecting wire is sufficient.

During the IR operation, the direction of the needle should be adjusted to the value decided in the planning phase. However, the surgeon cannot often look at the needle directly because Zerobot is controlled remotely. Even if the needle could be sighted, fine adjustments of the direction of the needle are difficult to achieve. Therefore, the actual direction of the needle should be shown intelligibly to the surgeon. To achieve this, the navigation display, which shows the direction of the needle to the surgeon by using a picture, was developed. The navigation display showing the picture is illustrated in **Fig. 7**. The two lines that are shown in **Fig. 7** indicate the direction of the needle. The three-dimensional (3D) information of the needle direction is depicted by the two lines in the two-dimensional (2D) plane. The line on left half of the picture corresponds to the angle of the needle on the CT image. The line on the right side of the picture corresponds to the angle of the needle on the plane, which is perpendicular to the CT radiography plane. The surgeon can confirm the direction of the needle by observing the lines and the displayed angles in order to adjust the direction of the needle to the preplanned angle. Concurrently, each display presents the value obtained from the force sensor on its plane. From this value, the surgeon can obtain the force due to needle insertion.

3. Kinematic Analysis

In order to establish remote center control, it requires the knowledge of the forward kinematics and inverse kinematics, which depends on the structure of the robot. The derivations of the forward and inverse kinematics are explained in this section. Zerobot has six active joints and a semi-fixed joint as shown in **Fig. 4**. The positive direction of each axis is represented by arrows. The semi-fixed axis is set to -90° or $+90^\circ$ as shown in **Fig. 8**. The angle (in $^\circ$) or displacement (in mm) of the six active axes is defined as $\boldsymbol{q} = [q_1, q_2, \ldots, q_6]^T$. The notations q_1, q_2, q_3 and q_6 represent linear axes, and q_4 and q_5 represent rotational axes. The position of the tip of the needle and the posture of the needle are defined as ${}^0\boldsymbol{r}_E = [x, y, z, \phi_A, \phi_B]^T$ where ϕ_A and ϕ_B are defined as in **Fig. 8**. ϕ_A is the angle of the needle on the CT radiography plane, and ϕ_B is the elevation angle of the plane. Forward kinematics is the projection of a vector from $\boldsymbol{q}$ to ${}^0\boldsymbol{r}_E$, and inverse kinematics is the projection of a vector from ${}^0\boldsymbol{r}_E$ to $\boldsymbol{q}$. Hereafter, $\sin\theta$ is represented as S_θ and $\cos\theta$ as C_θ. It should be noted that, originally, the elements of C_{α_3} are included in all the equations of kinematics (α_3 is defined in the following subsection). However, α_3 can take only $+90^\circ$ or -90°. In this case, the value of C_{α_3} must be zero. Therefore, in this study, the elements of C_{α_3} are omitted from all the equations of kinematics.

3.1. Forward Kinematics

The forward kinematics of Zerobot are derived by using Denavit-Hartenberg notation (DH notation) [10]. The location of the coordinate systems is shown in **Fig. 9**. These coordinate systems are located according to DH notation. The DH parameters are listed in **Table 1**. In the table, the value of α_3 depends on the direction of the semi-fixed axis. The required parameters l_1, l_2 and l_3 are defined in **Fig. 9**. Therefore, we can calculate ${}^0\boldsymbol{T}_6$, which is a homogeneous transformation matrix from Σ_0 to Σ_6. In addition, ${}^6\boldsymbol{T}_E$ is just a translational transformation matrix depending on the needle length, l_E. Therefore, ${}^0\boldsymbol{T}_E$ can be calculated as follows.

$$
{}^0\boldsymbol{T}_E = \begin{bmatrix} -S_{q_4}S_{q_5}S_{\alpha_3} & C_{q_4}S_{\alpha_3} & S_{q_4}C_{q_5}S_{\alpha_3} & {}^0r_{Ex} \\ C_{q_5}S_{\alpha_3} & 0 & S_{q_5}S_{\alpha_3} & {}^0r_{Ey} \\ C_{q_4}S_{q_5} & S_{q_4} & -C_{q_4}C_{q_5} & {}^0r_{Ez} \\ 0 & 0 & 0 & 1 \end{bmatrix} \quad (1)
$$

$$
\begin{aligned}
{}^0r_{Ex} &= l_3 - q_3 + l_2 S_{q_4} S_{\alpha_3} + q_6 S_{q_4} C_{q_5} S_{\alpha_3} + l_E S_{q_4} C_{q_5} S_{\alpha_3} \\
{}^0r_{Ey} &= q_6 S_{q_5} S_{\alpha_3} + q_2 - l_1 S_{\alpha_3} + l_E S_{q_5} S_{\alpha_3} \\
{}^0r_{Ez} &= q_1 - l_2 C_{q_4} - q_6 C_{q_4} C_{q_5} - l_E C_{q_4} C_{q_5}
\end{aligned}
$$

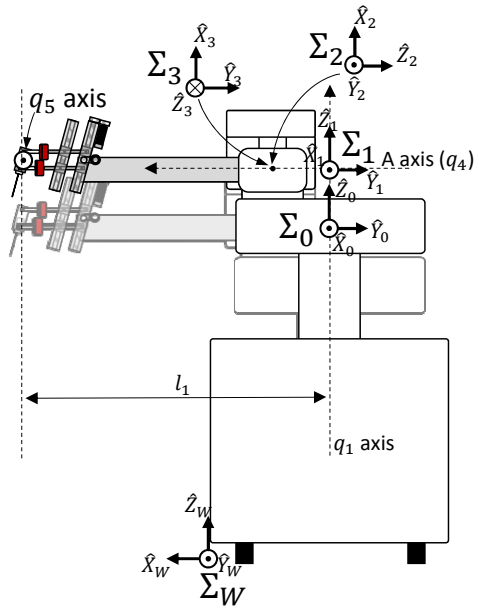

(a) Side view

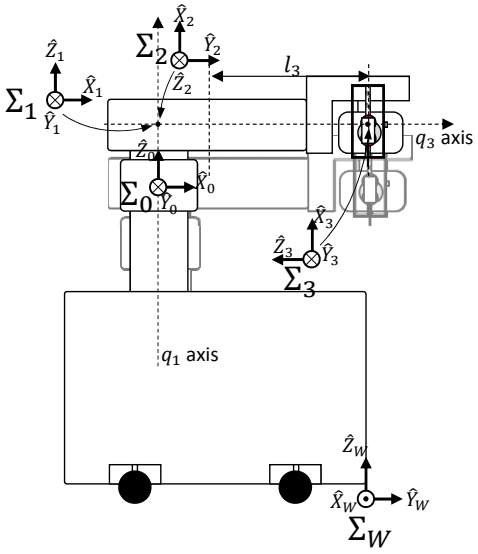

(b) Front view

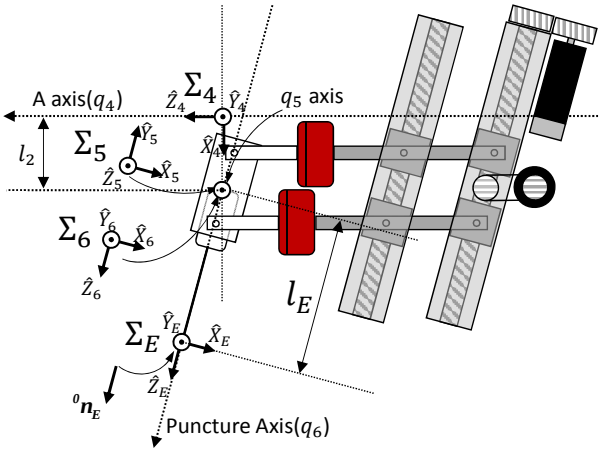

(c) End effector

Fig. 9. Location of coordinate systems.

Table 1. DH parameters.

i	α_{i-1}	a_{i-1}	d_i	θ_i
1	0	0	q_1	0
2	-90	0	q_2	-90
3	90	0	$q_3 - l_3$	0
4	90 or -90	0	l_1	$180 + q_4$
5	-90	l_2	0	$90 + q_5$
6	90	0	q_6	0

Next, ϕ_A and ϕ_B, which correspond to the needle posture, should be calculated. Then, the direction vector of the needle represented in Σ_0 is defined as ${}^0\boldsymbol{n}_E$. ${}^0\boldsymbol{n}_E$ is the same as the third column direction vector of the rotation matrix, ${}^0\boldsymbol{T}_E$. Therefore, ${}^0\boldsymbol{n}_E$ is represented as follows.

$$ {}^0\boldsymbol{n}_E = \begin{bmatrix} S_{q_4}C_{q_5}S_{\alpha_3} & S_{q_5}S_{\alpha_3} & -C_{q_4}C_{q_5} \end{bmatrix}^T \quad . \quad . \quad . \quad (2) $$

Here, ${}^0\boldsymbol{n}_E$ can also be represented using the notations ϕ_A and ϕ_B as follows. When we include ϕ_A and ϕ_B to the rotation matrix, which can change direction of Z-axis of Σ_0 same as that of $\hat{Z}_E$, the third column direction vector of the rotation matrix is ${}^0\boldsymbol{n}_E$.

$$ \begin{aligned} {}^0\boldsymbol{n}_E &= \begin{bmatrix} 1 & 0 & 0 \\ 0 & -1 & 0 \\ 0 & 0 & -1 \end{bmatrix} \cdot \begin{bmatrix} S_{\alpha_3} & 0 & 0 \\ 0 & S_{\alpha_3} & 0 \\ 0 & 0 & 1 \end{bmatrix} \\ &\quad \cdot \begin{bmatrix} 1 & 0 & 0 \\ 0 & C_{\phi_B} & -S_{\phi_B} \\ 0 & S_{\phi_B} & C_{\phi_B} \end{bmatrix} \cdot \begin{bmatrix} C_{\phi_A} & 0 & S_{\phi_A} \\ 0 & 1 & 0 \\ -S_{\phi_A} & 0 & C_{\phi_A} \end{bmatrix} \cdot \begin{bmatrix} 0 \\ 0 \\ 1 \end{bmatrix} \\ &= \begin{bmatrix} S_{\alpha_3}S_{\phi_A} \\ S_{\alpha_3}C_{\phi_A}S_{\phi_B} \\ -C_{\phi_A}C_{\phi_B} \end{bmatrix} \quad . \quad . \quad . \quad . \quad . \quad . \quad . \quad . \quad . \quad . \quad . \quad (3) \end{aligned} $$

By comparing Eqs. (2) and (3), we can calculate ϕ_A and ϕ_B shown in Eqs. (4) and (5).

$$ \phi_B = \tan^{-1}\left(\frac{1}{C_{q_4}}\tan q_5\right) \quad . \quad . \quad . \quad . \quad . \quad . \quad . \quad . \quad . \quad (4) $$

$$ \phi_A = \tan^{-1}\left(C_{\phi_B}\tan q_4\right) \quad . \quad . \quad . \quad . \quad . \quad . \quad . \quad . \quad . \quad (5) $$

Finally, ${}^0\boldsymbol{r}_E$ is calculated as follows.

$$ {}^0\boldsymbol{r}_E = \begin{bmatrix} l_3 - q_3 + l_2S_{q_4}S_{\alpha_3} + q_6S_{q_4}C_{q_5}S_{\alpha_3} + l_ES_{q_4}C_{q_5}S_{\alpha_3} \\ q_6S_{q_5}S_{\alpha_3} + q_2 - l_1S_{\alpha_3} + l_ES_{q_5}S_{\alpha_3} \\ q_1 - l_2C_{q_4} - q_6C_{q_4}C_{q_5} - l_EC_{q_4}C_{q_5} \\ \tan^{-1}\left(C_{\phi_B}\tan q_4\right) \\ \tan^{-1}\left(\frac{1}{C_{q_4}}\tan q_5\right) \end{bmatrix} \quad (6) $$

3.2. Inverse Kinematics

In this subsection, the procedure for deriving the inverse kinematics is described. The target position of the tip of the needle is defined as ${}^0\boldsymbol{r}_E^* = [x^*, y^*, z^*, \phi_A^*, \phi_B^*]^T$.

The target posture of the robot is defined as $\boldsymbol{q}^* = \left[q_1^*, q_2^*, \ldots, q_6^*\right]^T$. According to Eq. (6), the relationship between $\boldsymbol{q}^*$ and ${}^0\boldsymbol{r}_E^*$ is represented as follows.

$$\phi_B^* = \tan^{-1}\left(\frac{1}{C_{q_4^*}}\tan q_5^*\right) \quad \ldots\ldots\ldots (7)$$

$$\phi_A^* = \tan^{-1}\left(C_{\phi_B^*}\tan q_4^*\right) \quad \ldots\ldots\ldots (8)$$

$$x^* = (l_E + q_6) S_{q_4^*} C_{q_5^*} S_{\alpha_3} + l_2 S_{q_4^*} S_{\alpha_3} + l_3 - q_3^* \quad \ldots (9)$$

$$y^* = (l_E + q_6) S_{q_5^*} S_{\alpha_3} - l_1 S_{\alpha_3} + q_2^* \quad \ldots\ldots (10)$$

$$z^* = q_1^* - l_2 C_{q_4^*} - (l_E + q_6) C_{q_4^*} C_{q_5^*} \quad \ldots\ldots (11)$$

The inverse kinematics can be derived from Eqs. (7)–(11). However, Zerobot has redundant DOFs. Therefore, we derived the inverse kinematics assuming a fixed puncture axis (q_6 axis). The inverse kinematics are derived as follows.

$$q_4^* = \tan^{-1}\left(\frac{1}{C_{\phi_B^*}}\tan\phi_A^*\right) \quad \ldots\ldots\ldots (12)$$

$$q_5^* = \tan^{-1}\left(C_{q_4^*}\tan\phi_B^*\right) \quad \ldots\ldots\ldots (13)$$

$$q_1^* = z^* + l_2 C_{q_4^*} + (l_E + q_6) C_{q_4^*} C_{q_5^*} \quad \ldots\ldots (14)$$

$$q_2^* = l_1 S_{\alpha_3} - (l_E + q_6) S_{q_5^*} S_{\alpha_3} + y^* \quad \ldots\ldots (15)$$

$$q_3^* = l_2 S_{q_4^*} S_{\alpha_3} + (l_E + q_6) S_{q_4^*} C_{q_5^*} S_{\alpha_3} + l_3 - x^* \quad (16)$$

4. Evaluation Experiment

In this section, the experiment for evaluating the kinematics is described. The devices used in the experiment are listed below.

- Zerobot
- Laser sensor (Keyence Corp. TM-065)
- Dolly block (aluminum frame)

The configuration of the devices is illustrated in **Fig. 10(a)**. In order to fix the positional relation between Zerobot and laser sensor, the laser sensor is fixed to an aluminum frame. Using the laser sensor, we can get a binary image as shown in **Fig. 10(b)**. The position of the tip of the needle can be measured from the binary image. The experimental method is described as follows. In the actual robotic IR surgery, remote center control is used for the fine adjustment of the direction of the needle. We considered that the fine adjustment of the direction of the needle could be performed within a range of $\pm 10°$. Therefore, in this experiment, the range is increased slightly, and the operating range of ϕ_A is set to $-14° \leq \phi_A \leq 14°$. The operating interval is set to 2°. Under these conditions, Zerobot is remote center controlled by using inverse kinematics. The experimental conditions are illustrated in **Fig. 11**. The control system is illustrated in **Fig. 12**. Under these experimental conditions, the positioning accuracy of the tip of the needle is evaluated.

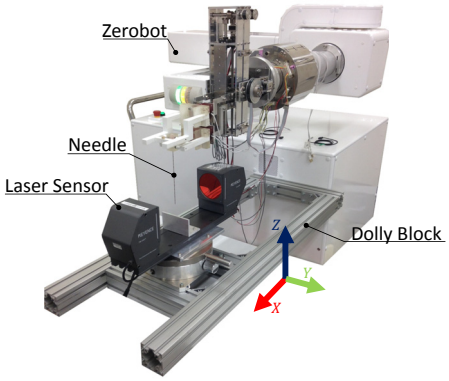

(a) Location of devices

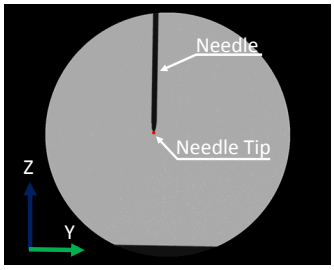

(b) Needle in sensor image

Fig. 10. Environment of evaluation experiment described in Section 4.

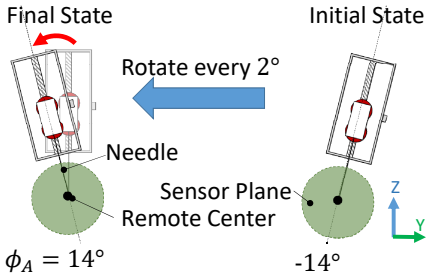

Fig. 11. Method of evaluation experiment of needle tip position.

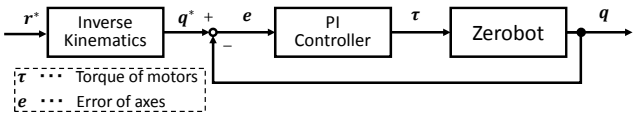

Fig. 12. Control system of Zerobot used in evaluation experiment.

4.1. Results

The experimental data is shown in **Figs. 13–14** and **Table 2**. **Fig. 13** is the superimposed sensor images of the needle. From this figure, it is confirmed that the trajectory of the needle is fan shaped. Therefore, the robot could rotate the needle accurately by fixing the position of the tip of the needle. **Fig. 14** shows the graph in which the position of the tip of the needle is plotted in all angles. All the plotted points lie within a circle of diameter 1.0 mm. Therefore, the target positioning accuracy of the tip of the needle is achieved.

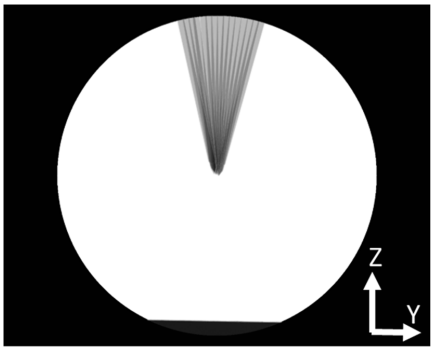

Fig. 13. Superimposed sensor images.

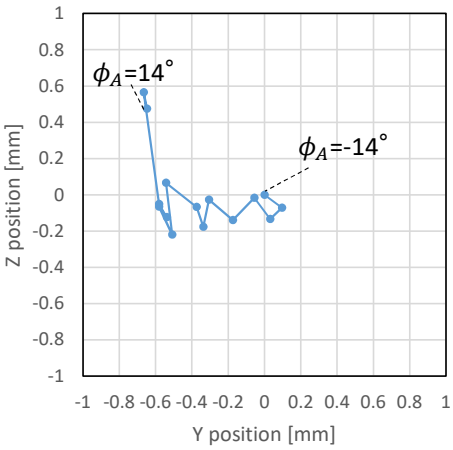

Fig. 14. Needle tip position.

Table 2. Results of experiment.

Target angle	Y position [mm]	Z position [mm]	Measured angle [°]
−14.0	0.17	−0.115	−13.84
−12.0	0.267	−0.187	−11.72
−10.0	0.201	−0.248	−9.99
−8.0	0.114	−0.131	−7.88
−6.0	−0.005	−0.254	−5.99
−4.0	−0.136	−0.142	−3.79
−2.0	−0.167	−0.292	−1.86
0.0	−0.204	−0.182	0.42
2.0	−0.372	−0.049	2.3
4.0	−0.338	−0.334	4.11
6.0	−0.411	−0.18	6.24
8.0	−0.368	−0.238	8.17
10.0	−0.411	−0.165	10.09
12.0	−0.495	0.45	12.11
14.0	−0.478	0.36	14.15
Max	0.267	0.45	
Min	−0.495	−0.334	
Max − Min	0.762	0.784	

Table 3. Accuracy of each axis of Zerobot.

Axis	q_1	q_2	q_3
Standard deviation	0.035 mm	0.036 mm	0.010 mm
	q_4	q_5	q_6
	0.011°	0.028°	0.026 mm

Table 4. Reproducibility of reattaching needle.

Axis	X	Y	Z
Standard deviation	0.064 mm	0.082 mm	0.223 mm

4.2. Discussion

In this experiment, the target positioning accuracy of the tip of the needle is achieved. According to **Table 2**, the Y position decreases gradually with the rotation of the needle. In addition, the Z position varies by approximately 0.8 mm. In order to verify this result, we conducted two preliminary experiments by using the same laser sensor. First, the independent controlling accuracy of each axis was confirmed. After deciding origin point of each axis 25 times respectively, the standard deviation of the position of the tip of the needle was obtained. The standard deviation of the positioning accuracy of each axis is listed in **Table 3**. Second, the reproducibility of the position of the needle tip after reattaching the needle to the end effector was confirmed. The needle was reattached 10 times, and the 3D position of the tip of the needle was acquired every time the needle is reattached. Then the standard deviation of the position of the needle tip was calculated. The standard deviation of the reattached needle tip position is shown in **Table 4**. According to the results of the preliminary experiment, it can be concluded that there are other causes for the dispersion of the position of the needle tip during remote center control. Then, we assumed that these variations in the position of the tip of the needle were caused by the mismatch in the center of rotation. From **Fig. 13**, it can be observed that all the positions of the needle tip exist above the center of rotation. In this case, the trajectory of the position of the needle tip shows an upward convex shape. Therefore, the Y position of the tip of the needle is varied. The position of the tip of the needle increases suddenly between 10° and 12° with respect to the Z position. This phenomenon implies that a mismatch in the center of rotation existed not only on the puncture axis but also on the axis perpendicular to the direction of the needle. It can be considered that the mismatch in the center of rotation was caused by a distortion in the link, an inclination of the linear axes, or a deflection of the needle. However, according to the result of the experiment, the positioning accuracy of the tip of the needle was equal to the target value of 1.0 mm. We concluded that the accuracy was sufficient for an IR surgery assisted by Zerobot.

5. Conclusion

This paper presents an overview of robotic IR, a proposal for remote center control, and an experiment for evaluating the positioning accuracy of the tip of the needle in remote center control. In the experiment, the control system achieved the target accuracy in positioning the tip of the needle. The derived inverse kinematics were also evaluated. Accordingly, it was confirmed that this control method could be used in actual robotic IR surgeries.

Acknowledgements

This work was supported by MEXT KAKENHI Grant Number 13233919 and Research on Development of New Medical Devices 15652923 from Japan Agency for Medical Research and Development, AMED.

References:

[1] T. Hiraki, T. Kamegawa, T. Matsuno, and S. Kanazawa, "Development of a Robot for CT Fluoroscopy-guided Intervention: Free Physicians from Radiation," Jon J. Intervent. Radiol., Vol.20, pp. 375-381, 2014.

[2] T. Hiraki, H. Gobara, H. Mimura, S. Toyooka, H. Fujiwara, K. Yasui, Y. Sano, T. Iguchi, J. Sakurai, N. Tajiri, T. Mukai, Y. Matsui, and S. Kanazawa, "Radiofrequency Ablation of Lung Cancer at Okayama University Hospital: A Review of 10 Years of Experience," Acta. Med., Vol.65, No.5, pp. 287-297, Okayama, 2011.

[3] D. Staianovici, K. Cleary, A. Patriciu, D. Mazilu, A. Stanimir, N. Craciunoiu, V. Watson, and L. Kavoussi, "AcuBot: A Robot for Radiological Interventions," IEEE Trans. on Robotics and Automation, Vol.19, No.5, pp. 927-930, October 2003.

[4] B. Maurin, B. Bayle, O. Piccin, J. Gangloff, M. Mathelin, C. Doignon, P. Zanne, and A. Gangi, "A Patient-Mounted Robotic Platform for CT-Scan Guided Procedures," IEEE Trans. on Biomedical Engineering, Vol.55, No.10, October 2008.

[5] Y. Koethe, S. Xu, G. Velusamy, B. J. Wood, and A. M. Venkatesan, "Accuracy and efficacy of percutaneous biopsy and ablation using robotic assistance under computed tomography guidance: a phantom study," European Radiology, Vol.24, Issue 3, pp. 723-730, March 2013.

[6] S. Ikeda, C. T. Villagran, T. Fukuda, Y. Okada, F. Arai, M. Negoro, M. Hayakawa, and I. Takahashi, "Patient-Specific IVR Endovascular Simulator with Augmented Reality for Medical Training and Robot Evaluation," J. of Robotics and Mechatronics, Vol.20, No.3, 2008.

[7] Y. Kobayashi, J. Okamoto, and M. G. Fujie, "Position Control of Needle Tip Based on Physical Properties of Liver and Force Sensor," J. of Robotics and Mechatronics, Vol.18, No.2, pp. 167-176, 2006.

[8] H. Nakaya, T. Matsuno, T. Kamegawa, T. Hiraki, T. Inoue, A. Yanou, M. Minami, and A. Gofuku, "CT Phantom for Development of Robotic Interventional Radiology," IEEE/SICE Int. Symposium on System Integration, Chuo University, Tokyo, Japan, December 13-15, 2014.

[9] K. Sugiyama, T. Matsuno, T. Kamegawa, T. Hiraki, H. Nakaya, A. Yanou, and M. Minami, "Reaction Force Analysis of Puncture Robot for CT-guided Interventional Radiology in Animal Experiment," IEEE/SICE Int. Symposium on System Integration (SII), Nagoya, Japan, December 11-13, 2015.

[10] J. J. Craig, "Introduction to ROBOTICS – mechanics and control," Addison-Wesley, 1989.

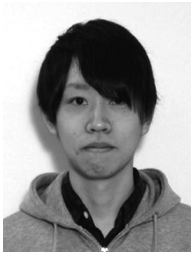

Name:
Kohei Sugiyama

Affiliation:
Student, Graduate School of Natural Science and Technology, Okayama University

Address:
3-1-1 Tsushimanaka, Kita-ku, Okayama city, Okayama 700-8530, Japan

Brief Biographical History:
2015- Graduate School of Natural Science and Technology, Okayama University

Main Works:
• medical robot

Name:
Takayuki Matsuno

Affiliation:
Lecturer, Graduate School of Natural Science and Technology, Okayama University

Address:
3-1-1 Tsushimanaka, Kita-ku, Okayama city, Okayama 700-8530, Japan

Brief Biographical History:
2000 Received M.E. degree from Nagoya University
2005 Received Dr.Eng. from Nagoya University
2004- Nagoya University
2006- Toyama Prefectural University
2011- Okayama University

Main Works:
• "Manipulation of Deformable Linear Objects using Knot Invariants to Classify the Object Condition Based on Image Sensor Information," IEEE/ASME Trans. on Mechatronics, Vol.11, Issue 4, pp. 401-408, 2006.
• "GPR Signal Processing with Geography Adaptive Scanning using Vector Radar for Antipersonal Landmine Detection," Int. J of Advanced Robotic Systems, Vol.4, No.2, pp. 199-206, 2007.

Membership in Academic Societies:
• The Institute of Electrical and Electronics Engineers (IEEE) Robotics and Automation Society (RAS)
• The Japan Society of Mechanical Engineers (JSME)
• The Robotics Society of Japan (RSJ)
• The Society of Instrument and Control Engineers (SICE)

Name:
Tetsushi Kamegawa

Affiliation:
Lecturer, Graduate School of Natural Science and Technology, Okayama University

Address:
3-1-1 Tsushimanaka, Kita-ku, Okayama city, Okayama 700-8530, Japan

Brief Biographical History:
1999/2001/2004 Received B.S., M.S. and Ph.D. degrees in Engineering from Tokyo Institute of Technology, respectively
2004 Visiting Scholar of Roma University
2004-2006 Researcher, International Rescue System Institute
2006-2009 Research Associate, Assistant Professor and Senior Assistant Professor, Okayama University

Main Works:
• snake robot and rescue robot

Membership in Academic Societies:
• The Japan Society of Mechanical Engineers (JSME)
• The Robotics Society of Japan (RSJ)
• The Society of Instrument and Control Engineers (SICE)

Name:
Takao Hiraki

Affiliation:
Associate Professor, Department of Radiology, Okayama University Hospital

Address:
2-5-1 Shikata, Kita-ku, Okayama city, Okayama 700-8558, Japan

Brief Biographical History:
1995 Received M.D. from Okayama University
2004- Joined Okayama University Hospital
2009- Assistant Professor, Okayama University Hospital
2012- Lecturer, Department of Radiology, Okayama University
2016- Associate Professor, Department of Radiology, Okayama University

Main Works:
• "Radiofrequency Ablation of Lung Cancer at Okayama University Hospital: A Review of 10 Years of Experience," Acta. Med., Vol.65, No.5, pp. 287-297, 2011.
• "Development of a Robot for CT Fluoroscopy-guided Intervention: Free Physicians from Radiation," Jon J. Intervent. Radiol., Vol.20, pp. 375-381, 2014.

Membership in Academic Societies:
• The Japanese Society of Interventional Radiology (JSIR)

Name:
Hirotaka Nakaya

Affiliation:
Student, Graduate School of Natural Science and Technology, Okayama University

Address:
3-1-1 Tsushimanaka, Kita-ku, Okayama city, Okayama 700-8530, Japan

Brief Biographical History:
2016 Received M.S. degree in Engineering from Okayama University
2016- Joined Mitsubishi Electric Corporation

Main Works:
• medical robot

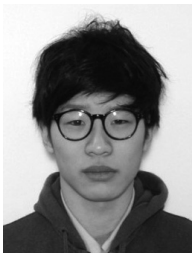

Name:
Masayuki Nakamura

Affiliation:
Student, Department of Mechanical Systems Engineering, Okayama University

Address:
3-1-1 Tsushimanaka, Kita-ku, Okayama city, Okayama 700-8530, Japan

Brief Biographical History:
2016 Received B.S. degree in Engineering from Okayama University
2016- Department of Mechanical Engineering, School of Engineering, Tokyo Institute of Technology

Main Works:
• medical robot

Name:
Akira Yanou

Affiliation:
Associate Professor, Department of Radiological Technology, Kawasaki College of Allied Health Professions

Address:
316 Matsushima, Kurashiki, Okayama 701-0194, Japan

Brief Biographical History:
2001 Received Ph.D. in Engineering from Okayama University
2002- Assistant Professor, Faculty of Engineering, Kinki University
2004- Lecturer, Faculty of Engineering, Kinki University
2009- Assistant Professor, Graduate School of Natural Science and Technology, Okayama University
2016- Associate Professor, Department of Radiological Technology, Kawasaki College of Allied Health Professions

Main Works:
• "Autonomous docking control of visual-servo type underwater vehicle system aiming at underwater automatic charging," Trans. of the JSME, Vol.81, No.832, 15-00391, Dec. 2015 (in Japanese).

Membership in Academic Societies:
• The Institute of Electrical and Electronics Engineers (IEEE)
• The Japan Society of Mechanical Engineers (JSME)
• The Society of Instrument and Control Engineers (SICE)
• The Institute of Systems, Control and Information Engineers (ISCIE)
• Japanese Society of Radiological Technology (JSRT)

Name:
Mamoru Minami

Affiliation:
Professor, Graduate School of Natural Science and Technology, Okayama University

Address:
3-1-1 Tsushimanaka, Kita-ku, Okayama city, Okayama 700-8530, Japan

Brief Biographical History:
1978/1980 Received B.S. and M.S. degrees in Aeronautical Engineering from University of Osaka Prefecture
1992 Received Ph.D. degree in Faculty of Engineering from Kanazawa University
1994- Associate Professor, Mechanical Engineering, University of Fukui
1999- Associate Professor, Department of Human and Artificial Intelligence Systems, University of Fukui
2002- Professor, University of Fukui
2010- Professor, Graduate School of Natural Science and Technology, Okayama University

Main Works:
• robotics and automation in dynamics, kinematics and control of robots including mobile manipulators, and intelligent motion control
• To research intelligent robot, he has been engaged in machine vision for real-time adaptive operation.

Membership in Academic Societies:
• The Japan Society of Mechanical Engineers (JSME)
• The Robotics Society of Japan (RSJ)
• The Society of Instrument and Control Engineers (SICE)
• The Institute of Electrical and Electronics Engineers (IEEE)